

SIMULATION OF TIDAL FLOW AND CIRCULATION PATTERNS IN
THE LOXAHATCHEE RIVER ESTUARY, SOUTHEASTERN FLORIDA

By Gary M. Russell and Carl R. Goodwin

U.S. GEOLOGICAL SURVEY

Water-Resources Investigations Report 87-4201

Prepared in cooperation with the

FLORIDA DEPARTMENT OF ENVIRONMENTAL REGULATION,
SOUTH FLORIDA WATER MANAGEMENT DISTRICT, PALM
BEACH COUNTY, MARTIN COUNTY, JUPITER INLET DISTRICT,
LOXAHATCHEE RIVER ENVIRONMENTAL CONTROL DISTRICT,
TOWN OF JUPITER, VILLAGE OF TEQUESTA, JUPITER INLET
COLONY, and the U.S. ARMY CORPS OF ENGINEERS

Tallahassee, Florida

1987

DEPARTMENT OF THE INTERIOR
DONALD PAUL HODEL, Secretary
U.S. GEOLOGICAL SURVEY
Dallas L. Peck, Director

For additional information
write to:

District Chief
U.S. Geological Survey
Suite 3015
227 North Bronough Street
Tallahassee, Florida 32301

Copies of the report can be
purchased from:

U.S. Geological Survey
Books and Open-File Reports Section
Federal Center, Building 810
Box 25425
Denver, Colorado 80225

CONTENTS

	Page
Abstract-----	1
Introduction-----	1
Purpose and scope-----	1
Approach-----	2
Description of study area-----	2
Model description-----	4
Input requirements-----	5
Assumptions and limitations-----	5
Model development-----	6
Boundary conditions-----	6
Initial conditions-----	8
Calibration-----	8
Tidal stage-----	10
Tidal velocity-----	17
Distribution of tidal-flow volumes-----	17
Verification-----	17
Tidal flow and circulation patterns-----	20
Ebb transport-----	20
Flood transport-----	20
Near-slack transport-----	25
Residual transport-----	25
Summary and conclusions-----	30
References cited-----	31
Glossary-----	32

ILLUSTRATIONS

Figure 1. Map showing Loxahatchee River estuary streamflow, tidal-stage, and velocity measurement sites-----	3
2. Map showing orientation of the Loxahatchee River estuary model-----	7
3. Graph showing effects of changes in the shape and cross-sectional area at site 1 near Jupiter Inlet, February 25, 1975-----	9
4. Graph showing range and phase as a function of distance for various frictional coefficients in the Loxahatchee River estuary-----	11
5-8. Graphs showing comparisons of observed and computed tidal stage:	
5. Near Jupiter Inlet, (A) site 1, (B) site 4-----	12
6. Near the Florida East Coast Railroad bridge at site 8-----	13
7. In the northwest fork and in the southwest fork, (A) site 12, (B) site 11-----	14
8. In the northwest fork, (A) site 15, (B) site 14-----	15

ILLUSTRATIONS--Continued

	Page
Figure 9. Graphs showing comparisons of observed and computed velocities, (A) site 2, (B) site 8, (C) site 9, (D) site 10, (E) site 13, (F) site 15-----	18
10-15. Maps showing water transports:	
10. In the central embayment during ebb tide-----	21
11. From Jupiter Inlet to the central embayment during ebb tide-----	22
12. In the central embayment during flood tide-----	23
13. From Jupiter Inlet to the central embayment during flood tide-----	24
14. In the central embayment during near-slack tide-----	26
15. From Jupiter Inlet to the central embayment during near-slack tide-----	27
16. Map showing residual water transport in the central embayment--	28
17. Map showing residual water transport from Jupiter Inlet to the central embayment-----	29

TABLES

Table 1. Summary of comparisons between observed and computed tidal stage and tidal phase at high and low tides in the Loxahatchee River estuary-----	16
2. Measured and computed distribution of tidal-flow volumes in the vicinity of Jupiter Inlet-----	19

CONVERSION FACTORS AND ABBREVIATIONS

For the convenience of readers who may prefer to use metric (International System) units, rather than the inch-pound terms used in this report, values may be converted by using the following factors:

<u>Multiply inch-pound unit</u>	<u>By</u>	<u>To obtain metric unit</u>
inch per month (in/mo)	25.4	millimeter per month (mm/mo)
foot (ft)	0.3048	meter (m)
foot per second (ft/s)	0.3048	meter per second (m/s)
square foot (ft ²)	0.09294	square meter (m ²)
cubic foot (ft ³)	0.02832	cubic meter (m ³)
cubic foot per second (ft ³ /s)	0.02832	cubic meter per second (m ³ /s)
mile (mi)	1.609	kilometer (km)
square mile (mi ²)	2.590	square kilometer (km ²)

Sea level: In this report "sea level" refers to the National Geodetic Vertical Datum of 1929 (NGVD of 1929)--a geodetic datum derived from a general adjustment of the first-order level nets of both the United States and Canada, formerly called "Mean Sea Level of 1929."

SIMULATION OF TIDAL FLOW AND CIRCULATION PATTERNS IN THE
LOXAHATCHEE RIVER ESTUARY, SOUTHEASTERN FLORIDA

By Gary M. Russell and Carl R. Goodwin

ABSTRACT

Results of a two-dimensional, vertically averaged, computer simulation model of the Loxahatchee River estuary show that under typical low freshwater inflow and vertically well-mixed conditions, water circulation is dominated by freshwater inflow rather than by tidal influence. The model can simulate tidal flow and circulation in the Loxahatchee River estuary under typical low freshwater inflow and vertically well-mixed conditions but is limited, however, to low-flow and well-mixed conditions. Computed patterns of residual water transport show a consistent seaward flow from the northwest fork through the central embayment and out Jupiter Inlet to the Atlantic Ocean. A large residual seaward flow was computed from the North Intracoastal Waterway to the inlet channel. Although the tide produces large flood and ebb flows in the estuary, tide-induced residual transport rates are low in comparison with freshwater-induced residual transport. Model investigations of partly mixed or stratified conditions in the estuary need to await development of systems capable of simulating three-dimensional flow patterns.

INTRODUCTION

Growing concern for the environmental health of the Loxahatchee River estuary by citizens and local, State, and Federal agencies led to an agreement in 1979 whereby the U.S. Geological Survey would conduct a cooperative investigation to provide information on physical, chemical, biological, and hydrologic conditions within the Loxahatchee River estuary (McPherson and Sabanskas, 1980). This report documents tidal flows and horizontal circulation patterns of the estuary. Results from other aspects of the investigation have been reported in several previous publications (McPherson and Sonntag, 1983; McPherson and Sonntag, 1984; McPherson and others, 1984; Sonntag and McPherson, 1984a; Sonntag and McPherson, 1984b; Wanless and others, 1984).

Water circulation is one of the most important physical processes that occurs in estuaries. It is also one of the most difficult processes to measure. Water circulation controls, or greatly affects, the distribution and flushing of dissolved and suspended waterborne constituents including salt, nutrients, dissolved oxygen, plankton, sediment, and trace elements and compounds.

Purpose and Scope

This report presents results from one objective of the overall study, which is to determine the patterns of two-dimensional tide-induced circulation in the Loxahatchee River estuary. The information is useful in

explaining the distribution of bottom sediments and waterborne constituents within the estuary.

The study area extends from nearshore regions of the Atlantic Ocean near Jupiter Inlet--the ocean entrance to the Loxahatchee River estuary--to the approximate upstream limit of tidal influence in the tributaries to the estuary (fig. 1). Parts of the Intracoastal Waterway, both north and south of Jupiter Inlet, are also within the study area.

Approach

The primary tool used to define water circulation in the Loxahatchee River estuary is a two-dimensional, vertically averaged, hydrodynamic numerical model that utilizes a high-speed computer to solve the system of equations. The model is capable of closely approximating water-level and water-velocity data in the prototype (real-world) system. Once the model is adjusted to adequately simulate the prototype, controlled numerical experiments can be conducted with the model. On the basis of experimental results, inferences can be made regarding how the prototype would respond to simulated field conditions.

A graphical comparison between model-computed data and observed stage, velocity, and tidal-flow distribution data from the prototype is used to determine the degree of model-to-prototype similarity. Prototype data were available from a one-dimensional model study by Chiu (1975) and from data collected as part of this study. These data include bathymetry, tidal stage, and tidal velocity in the estuary. Bathymetric data were obtained from the National Ocean Survey for depth information obtained in 1969. The U.S. Geological Survey resurveyed selected areas in 1980 and 1981 using depth-sounding equipment (McPherson and others, 1982). No extensive bottom changes were detected since the National Ocean Survey assessment except for dredged channels in the central embayment. Tidal stage and velocity data were obtained on February 26, 1975, by Chiu (1975), and by the U.S. Geological Survey on March 2-3, 1981. Simulation of water circulation in the Loxahatchee River estuary was based on assumptions of vertically well-mixed conditions. Partly mixed or density-stratified conditions were excluded from simulation analysis. Overall circulation patterns were displayed in computer-prepared maps that show water-transport vectors at computation points within the model.

Description of Study Area

The Loxahatchee River estuary is tributary to the Atlantic Ocean at Jupiter Inlet (fig. 1). The estuarine system comprises three forks: the southwest fork, north fork, and northwest fork. At a point 4.26 river miles upstream from the ocean (fig. 1), the northwest fork widens to form the western part of an embayment. At river mile 2.58, the north and southwest forks join to complete the irregularly shaped embayment that is about 3 miles long and averages about 0.5-mile wide. The eastern end of the embayment narrows at the location of the Florida East Coast Railroad (FECRR) bridge. A 1-mile section connecting the estuary to the ocean is a nearly straight channel culminating at Jupiter Inlet. The Intracoastal Waterway (fig. 1) is another

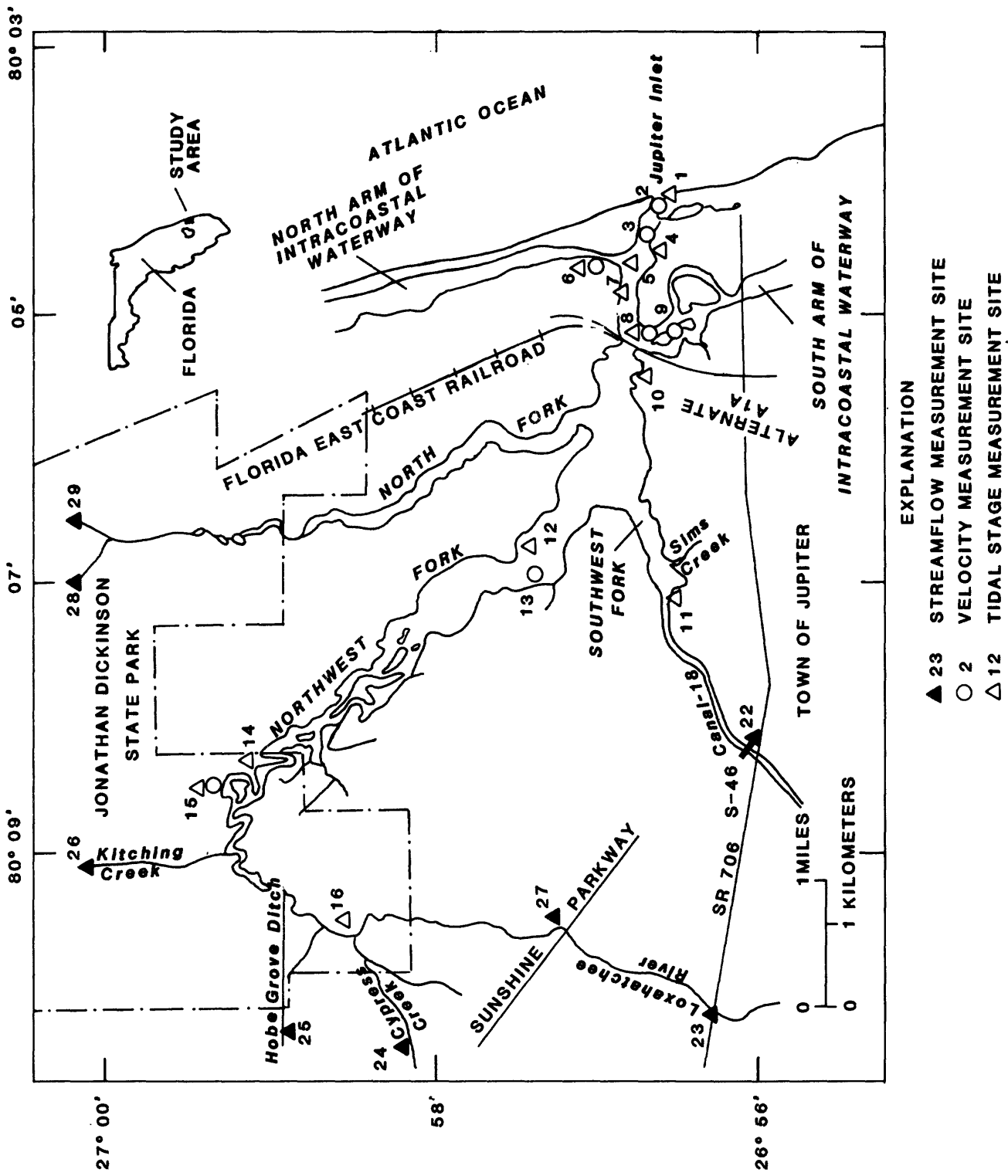


Figure 1.--Loxahatchee River estuary streamflow, tidal-stage, and velocity measurement sites.

feature of the estuarine system that extends both northward and southward from the 1-mile inlet channel segment.

Estuarine conditions extend from Jupiter Inlet to about 5 river miles up the southwest fork, 6 river miles up the north fork, and 10 river miles up the northwest fork. Four tributaries--Loxahatchee River, Cypress Creek, Hobe Grove Ditch, and Kitching Creek--discharge to the northwest fork (fig. 1). Canal-18 (C-18), built in 1957-58, is the major tributary to the southwest fork. The north fork has several small unnamed tributaries.

The Loxahatchee River estuary is shallow with an average depth of about 4 feet. Sandbars and oyster bars in the central embayment are occasionally exposed at low tide as is much of the forested flood plain in the northwest fork (McPherson and Sabanskas, 1980). Some deep parts of the estuary are a result of dredging (McPherson and others, 1982). In the northwest fork, a natural river channel, with maximum depths that range from about 10 to 20 feet, extends upstream near Cypress Creek. Farther upstream, maximum depths are generally less than 10 feet.

Rainfall in the study area is seasonal with 5 in/mo common during the wet season from May through October. Amounts near 2.5 in/mo generally occur during the dry season from November to April.

Freshwater inflow to the estuary during the wet season typically exceeds 120 ft³/s and is sufficient to cause density stratification throughout much of the estuary. The stratification generally persists until discharges moderate in late fall. During the dry season, tidal energy is adequate to overcome the density stratification, and the estuary can be vertically well mixed (Russell and McPherson, 1983, p. 27).

MODEL DESCRIPTION

The SIMSYS2D (two-dimensional estuarine-simulation system) model, described by Leendertse (1970) and applied by Goodwin (1977; 1980), was used in this study. The model requires overlying the active flow area with a rectangle grid having square cells. Bed-elevation, roughness, initial water-surface elevation, concentration, and density data are required at each cell. One or more cells are designated to add water to or remove water from the modeled area. The results are computed water levels, concentrations, and velocities at each cell at the end of each time step. The model uses a multi-operation, alternating-direction, implicit procedure to solve second-order finite-difference approximations to the time-dependent partial-differential equations representing conservation of mass and momentum in two-dimensional waterflow. The physical laws governing water motion in two dimensions are written in equation form for every cell in the active flow system. Solution of these equations produces synoptic water-level, water-velocity, and water-transport data throughout the modeled region at the end of each time step. A comprehensive presentation of the governing equations and numerical procedures may be found in Leendertse (1970) and Leendertse and Gritton (1971).

Input Requirements

Conceptually, two basic types of input data are needed to operate the SIMSYS2D estuarine-simulation system: (1) data that define conditions existing at the various model boundaries for the duration of the computational period (boundary conditions); and (2) data that define the physical characteristics of water within the estuary and its condition at the start of the computational period (initial conditions).

Boundary conditions that require definition include shape of the estuary, hydraulic roughness of bottom materials, location and rates of freshwater inflow, windspeed and direction over the water surface, and the time history of tidal velocity or tidal stage at the open boundaries of the model. Open boundaries are commonly located at tidal inlets or at some distance into an ocean, sea, or gulf. All boundary conditions can be measured directly in the prototype and used for model input except for bottom roughness. Bottom-roughness coefficients must be estimated and subsequently adjusted to achieve a similarity between model results and prototype conditions. Initial prototype conditions that require definition include water density, starting water-surface elevations, and water velocity.

Assumptions and Limitations

Important assumptions inherent in the SIMSYS2D modeling system and limitations imposed by application to the Loxahatchee River estuary are summarized below. Assumptions and limitations are discussed to provide insight on the accuracy of computed results and subsequent applicability of the model to the prototype.

One primary modeling assumption is that the water body under investigation is vertically well mixed (no density stratification). In the Loxahatchee River estuary, this indicates that model results are applicable to the prototype only during times of low freshwater inflow.

Model investigations also must establish a compromise between the number of computational cells and the frequency of computations with the cost of computer usage. The smaller the cell size (distance between computational cells) and the smaller the time step (time between computations), the greater the computational cost. In this application, a uniform cell size of 250 feet on each side and a time step of 3 minutes were considered adequate to both define flow and circulation in the central embayment, the area of primary interest, and to limit computer costs.

A major limitation of the 250-foot cell size is the lack of definition in narrow channels. This occurs in the upper reaches of the major tributaries where channel widths are less than the cell size. Also, the channel connecting the estuary and ocean is somewhat wider than 250 feet, but there is not sufficient subdivision to show the two-dimensional nature of the flow. The lack of definition in these areas is not believed to adversely affect the results.

MODEL DEVELOPMENT

Model development is a procedure whereby a prototype system is numerically approximated by adjustment of parameters representing processes affecting the state of the system so that model computations closely match observed data from the prototype system. Parameters represent system processes which have not been directly measured, or for which measurements contain a range of uncertainty large enough to affect model computations. The objective is to demonstrate that the model can compute values that are very similar to observed data.

If many sets of data representing various states of the system are available for this process of calibration, and a single set of parameters reproduces the system response to a reasonable degree of accuracy in all of them, some degree of confidence is acquired. The model will then reproduce the system response under hypothetical conditions for which no real data are available (predictions). Confidence is limited to conditions that are within the bounds of the test data sets. In this study, only one set of data was used for calibration. Data sets for different hydrologic conditions are needed to validate the predictive ability of the model.

Boundary Conditions

The modeled area of the Loxahatchee River estuary modeled with the SIMSYS2D estuarine-simulation system is shown in figure 2. The modeled area comprises 11.3 mi², about 79 percent of which is land above the elevation of mean high water. The cell dimension, 250 feet, resulted in a 47 by 107 matrix. The orientation of the rectangle enclosing the modeled area is rotated 30 degrees clockwise from the north to encompass as much of the estuary in as small a rectangle as possible to improve computational efficiency. Some bending or realignments of the three major tributaries (fig. 2) was justified to minimize the size of the model area.

Rotation of the model rectangle permitted extension of the seaward boundary into the Atlantic Ocean. This was beneficial because the ocean and inlet can interact naturally without excessive interference from an artificially imposed tidal-boundary condition. Interference can cause numerical instability, thus, preventing a solution to the test. Tidal stage was simulated at the boundary by using a sinusoid tide having an amplitude of 2.1 feet and a 12-hour period that closely approximated ocean tides, as reported by Chiu (1975) and as measured by the U.S. Geological Survey on March 2-3, 1981. Wind was set to zero. Both the North Intracoastal Waterway and the South Intracoastal Waterway were initially modeled as water-storage areas. Evaluation of early model results indicated that this assumption was adequate in the South Intracoastal Waterway probably because of low tidal velocity, but inadequate in the North Intracoastal Waterway because of higher velocity. A tidal boundary was established in the North Intracoastal Waterway that produced adequate results in subsequent simulations.

Water-depth values were assigned to each cell to define the estuary bottom. Land elevations for all cells above the approximate mean high-water line were assigned a default elevation of 3 feet. These assignments define

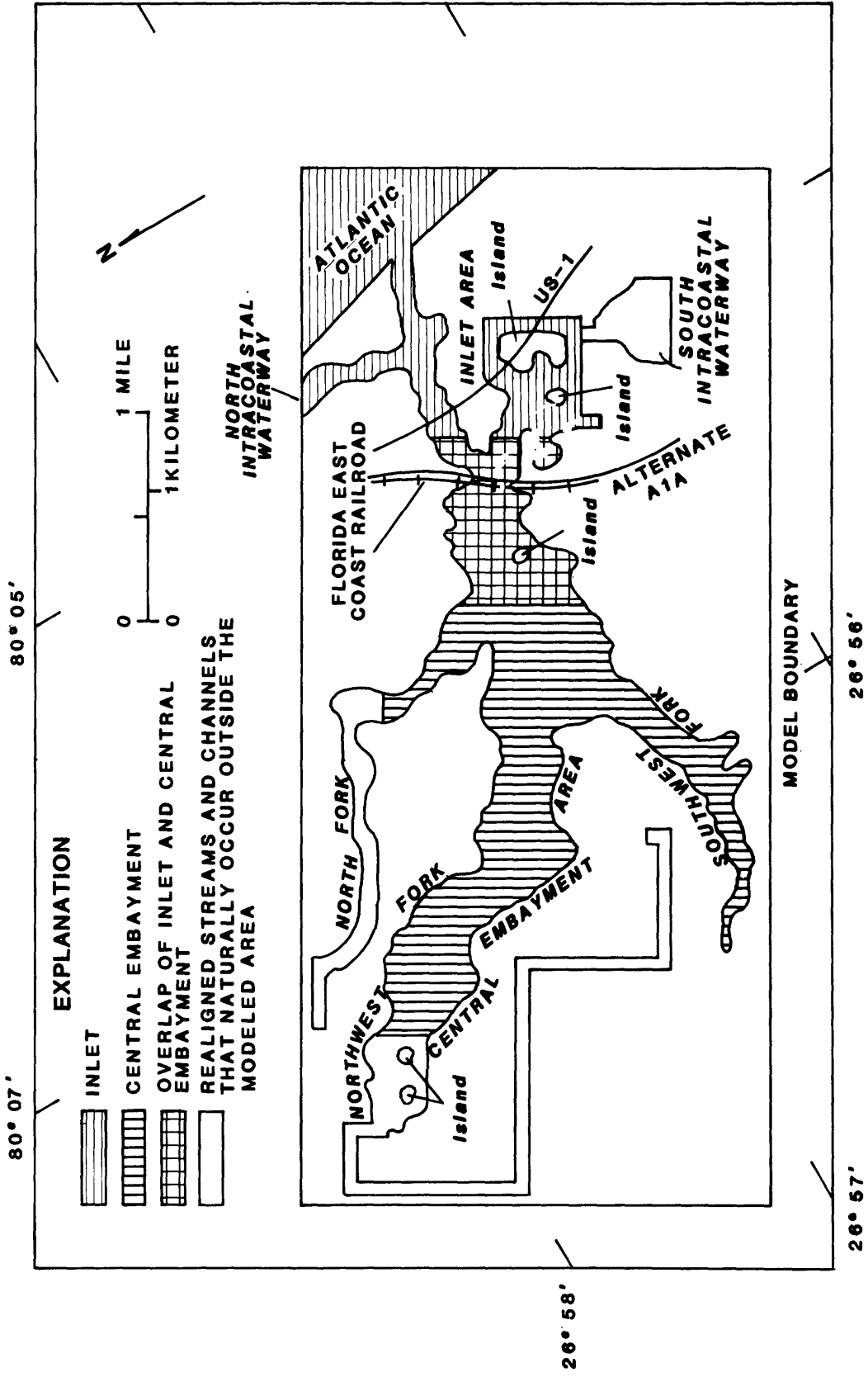


Figure 2.--Orientation of the Loxahatchee River estuary model.

the unique shape characteristics of the estuary that largely control how water is numerically distributed.

The estuary bottom was treated as a fixed impervious boundary which causes resistance to the free flow of water. This resistance increases as the roughness of bottom material increases. Hydraulic engineering practice in the United States has made extensive use of the Manning formulation for describing flow in open channels. This formulation includes a bottom roughness coefficient, "n" (Barnes, 1967). Values for Manning's roughness coefficient were assigned to each cell in the model.

The modeled shoreline was treated as a no-flow boundary except where tributary flow was inserted. Discharges for each tributary were computed from averages at U.S. Geological Survey gaging sites on the river (fig. 1) during the study period. Average tributary discharges were 120 ft³/s for the northwest fork and 15 ft³/s for the north fork (Russell and McPherson, 1983, p. 34). The model allows the shoreline boundary to migrate landward or seaward as water levels increase or decrease, respectively.

Initial Conditions

The initial water stage was uniform in all active cells and set equal to the elevation of the ocean at the seaward boundary. All velocities prior to each model run were assigned a value of zero so the initial water levels were flat, representing a stationary mass of water throughout the estuary. About 12 hours had to be simulated before the model was no longer influenced by the initial conditions. Model computations during this 12-hour period were disregarded. When a model run was restarted to extend the simulation, tidal stage and velocity conditions at each cell were read from a restart file created by the previous run, thus, no additional stabilization period was required.

Calibration

The model was calibrated using tidal-stage and velocity data obtained on February 25, 1975 (Chiu, 1975), from seven tidal-stage sites and four tidal-velocity sites between the Atlantic Ocean and the upper reaches of the northwest fork (fig. 1). Similar semidiurnal tide data observed by the U.S. Geological Survey on March 2-3, 1981, were obtained at six tidal-stage sites and four tidal-velocity sites and used to supplement Chiu's data. Distribution of tidal flow into and out of the various tributaries measured by Chiu (1975) and by the U.S. Geological Survey were also used in model calibration.

The model demonstrated that computed stages and flows within the estuary were very sensitive to small changes in the shape and cross-sectional areas of the entrance channel (fig. 3). Channel depths were adjusted between 10- and 12-foot depths below sea level. These changes in depths resulted in cross-sectional area differences between 3,375 and 5,400 ft². Cross-section D (5,000 ft²) achieved the best match between computed and observed data. Figure 3 can also be used to indicate how the tidal range within the estuary might change due to natural or manmade changes to the entrance channel.

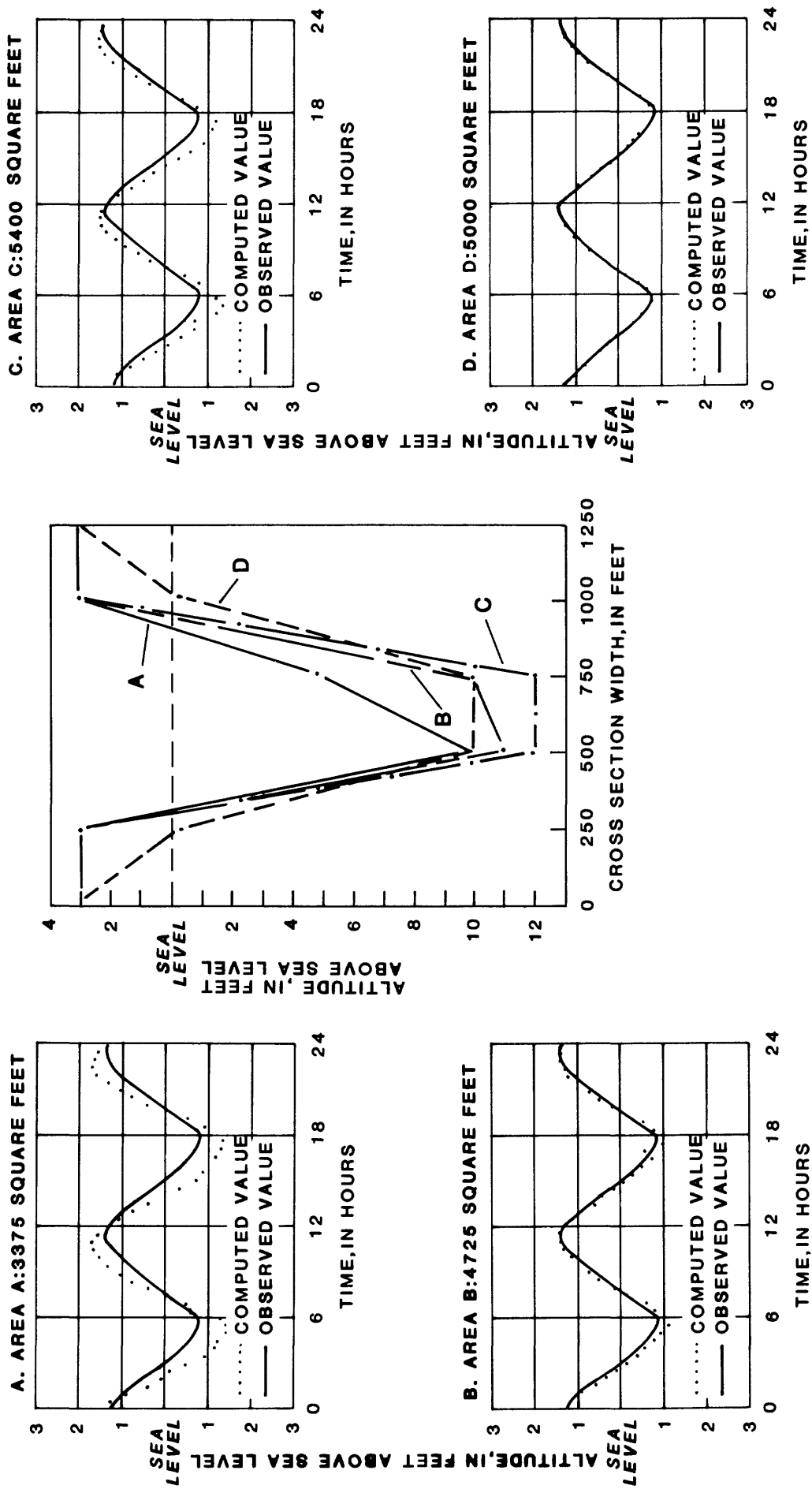


Figure 3.--Effects of changes in the shape and cross-sectional area at site 1 near Jupiter Inlet, February 25, 1975.

In a series of subsequent model runs, bottom roughness coefficients were selectively adjusted to provide as good a match as possible between measured and computed tidal data (fig. 4). During model calibration, "n" values ranged from 0.020 to 0.056. The best match was achieved at a roughness coefficient "n" value of 0.035. This value is in general agreement with published values for similar bottom conditions (Barnes, 1967). Local areas of known high resistance to flow such as oyster bars, seagrass beds, bridges, and piers were assigned roughness coefficients from 0.040 to 0.056.

Tidal Stage

Comparisons of computed and observed tidal-stage and tidal-phase data are shown in figures 5 through 8 and summarized in table 1. Site locations are shown in figure 1. Figure 5A shows the input tide at the open model boundary (fig. 1, site 1) and observed tides just outside Jupiter Inlet. No shift in tidal phase or amplitude was assumed to occur between the ocean boundary and the inlet entrance. Just inside the inlet (fig. 1, site 4), observed data and model results (fig. 5B) indicate a decrease in tidal range of about 50 percent and a phase lag of about 1 hour from tide data at the inlet. The average difference between computed and observed stage elevation is about 0.13 foot. Computed data compare well with observed data at site 4, indicating that the model properly simulated conditions at Jupiter Inlet.

Figure 6 compares observed and computed tidal-stage data during two time periods near the FECRR bridge (fig. 1, site 8). Data during March 1981 (fig. 6B) show high tide stage within 0.04 foot and low tide stage within 0.07 foot. Computed phase lags (table 1) differ from observed values by 10 minutes at high tide and by 25 minutes at low tide. In February 1975, data at site 8 (fig. 6A) had similar comparative characteristics. Calibration during both dates at this site is considered to be good.

Tidal stage and phase comparisons in the northwest fork (fig. 1, site 12) and the southwest fork (fig. 1, site 11) are shown in figure 7 (A and B, respectively). At both sites, the similarity between computed and observed data is considered to be only fair. At site 12, the stage comparisons at high and low tide are good, 0.01 and 0.09 foot, respectively. The phase-lag differences range from 40 to 45 minutes. At site 11, high- and low-stage comparisons are off by 0.20 and 0.18 foot, respectively. Phase-lag differences range from 10 to 20 minutes.

Figure 8 shows comparisons of observed and computed tidal-stage data at two sites in the northwest fork. Stage comparisons at high and low tide at site 14 are within 0.12 foot. Stage comparisons at site 15 are 0.11 foot at high tide and 0.08 foot at low tide. Whereas differences in tidal-stage comparison are good, comparison of differences in phase lag are poor. Phase-lag difference at both sites during high tide was 94 minutes and 118 minutes during low tide.

Lack of good comparisons between model and prototype stage data at sites 11 and 12 (fig. 7) and sites 14 and 15 (fig. 8) could be a result of several factors. Phase-lag differences tend to increase with distance from the inlet,

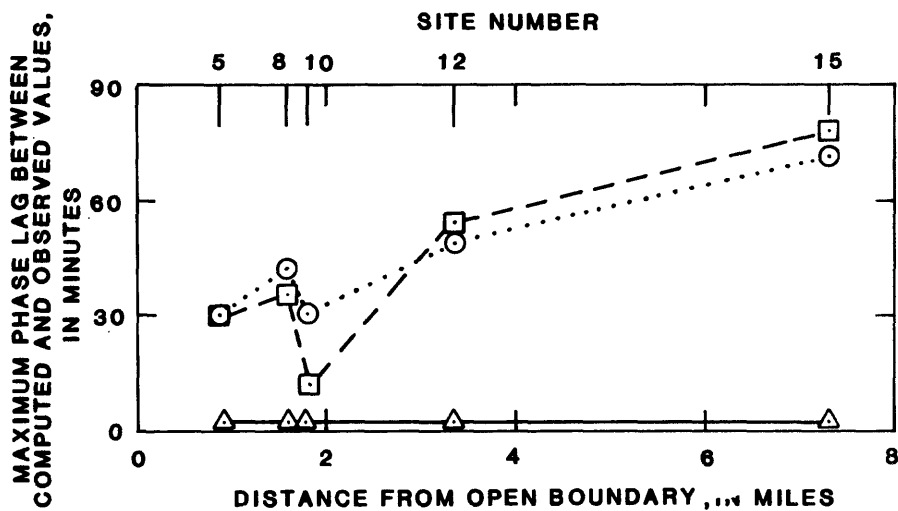
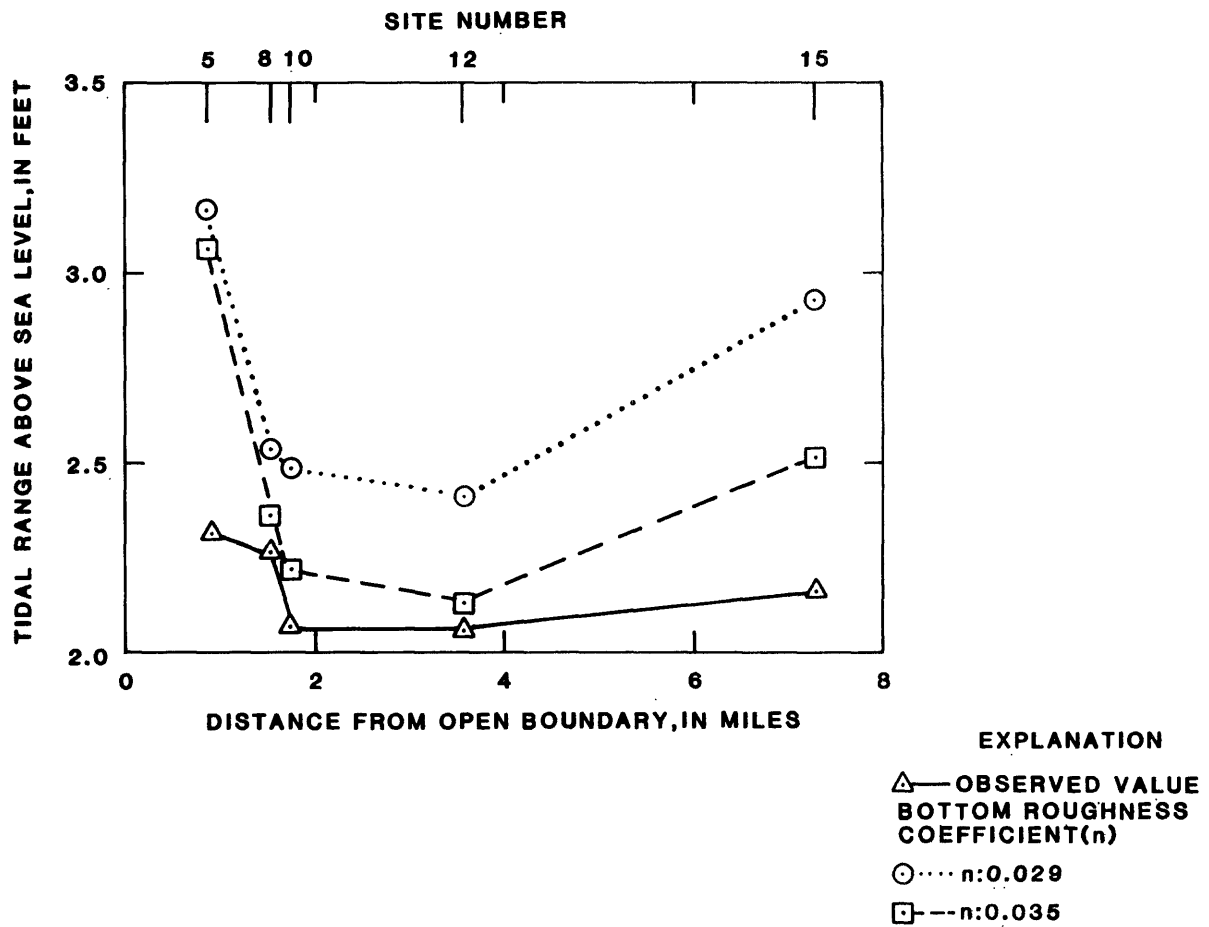


Figure 4.--Range and phase as a function of distance for various frictional coefficients in the Loxahatchee River estuary.

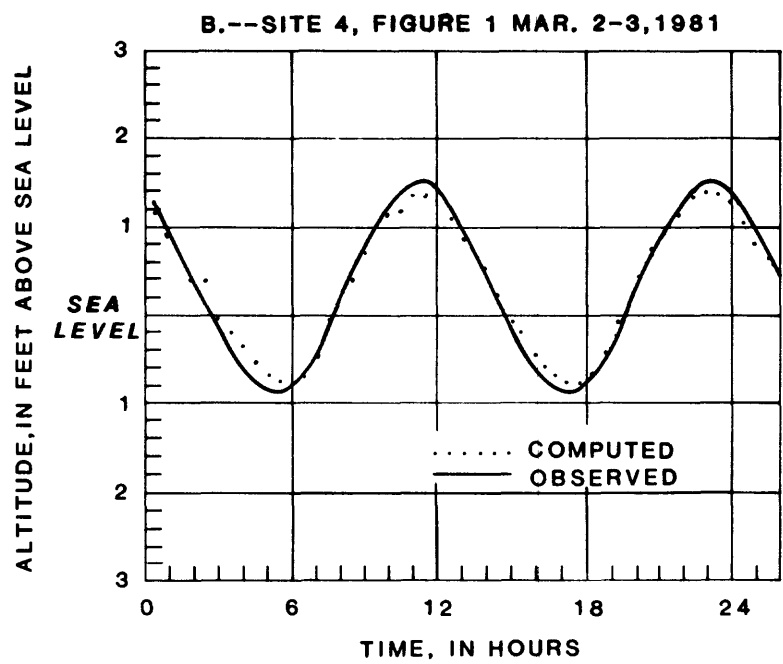
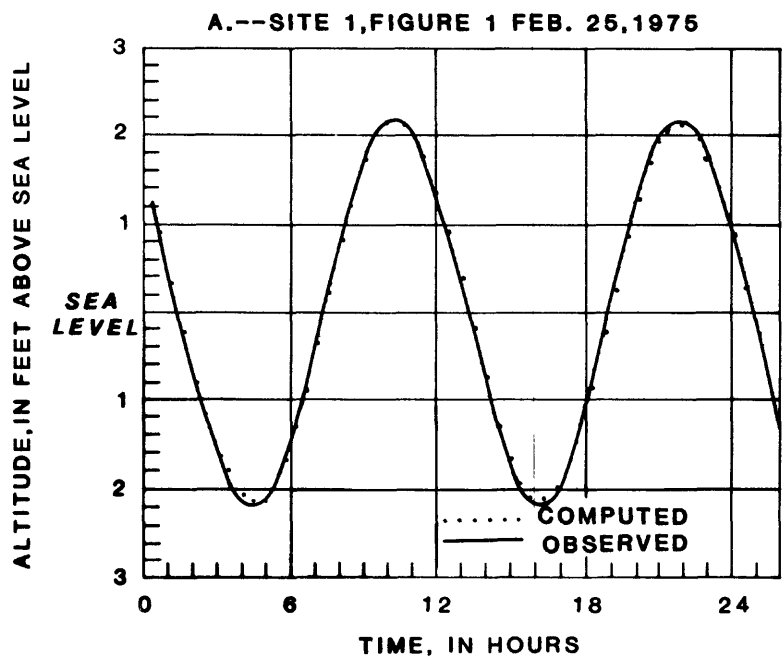


Figure 5.--Comparison of observed and computed tidal stage near Jupiter Inlet, (A) site 1, (B) site 4.

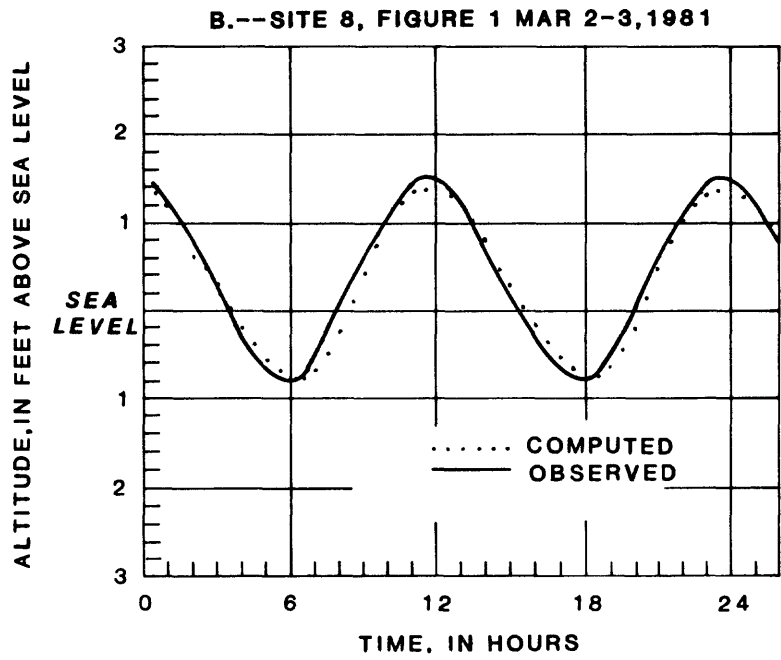
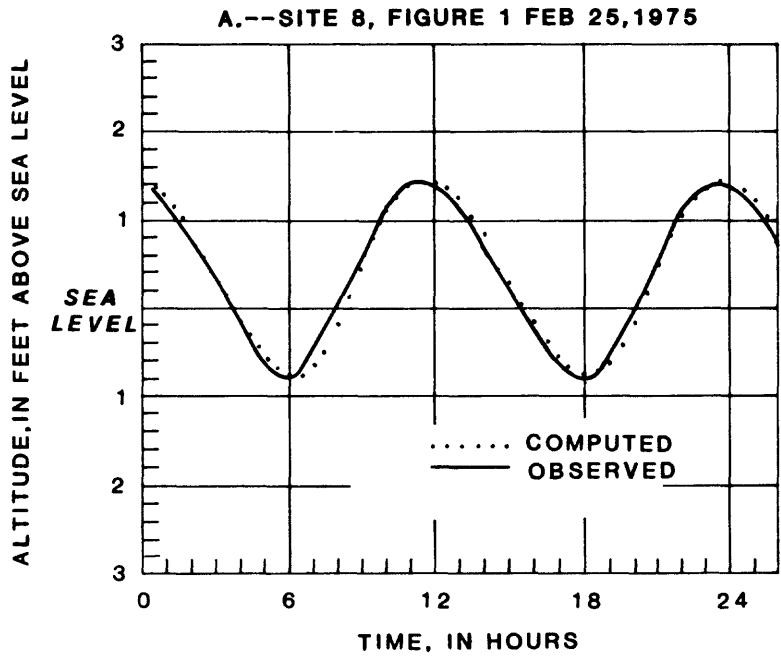


Figure 6.--Comparison of observed and computed tidal stage near the Florida East Coast Railroad bridge at site 8.

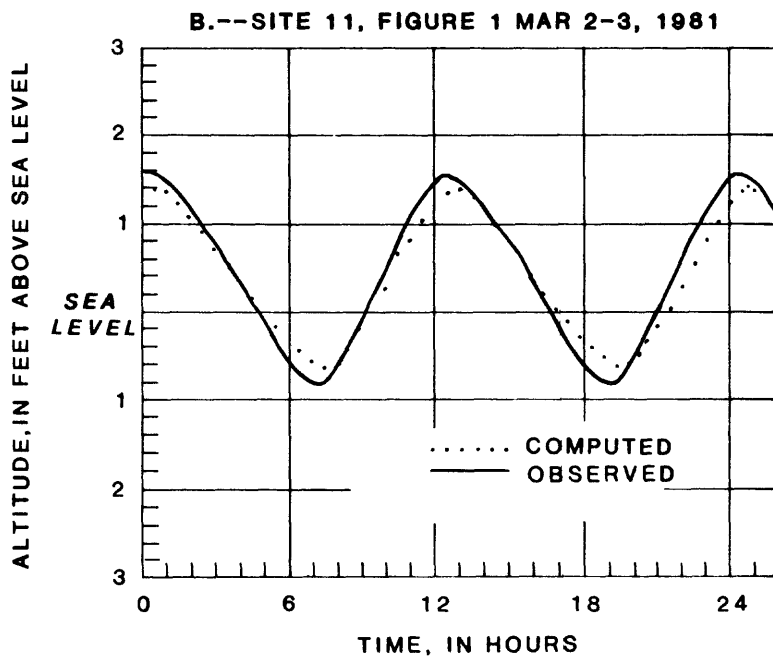
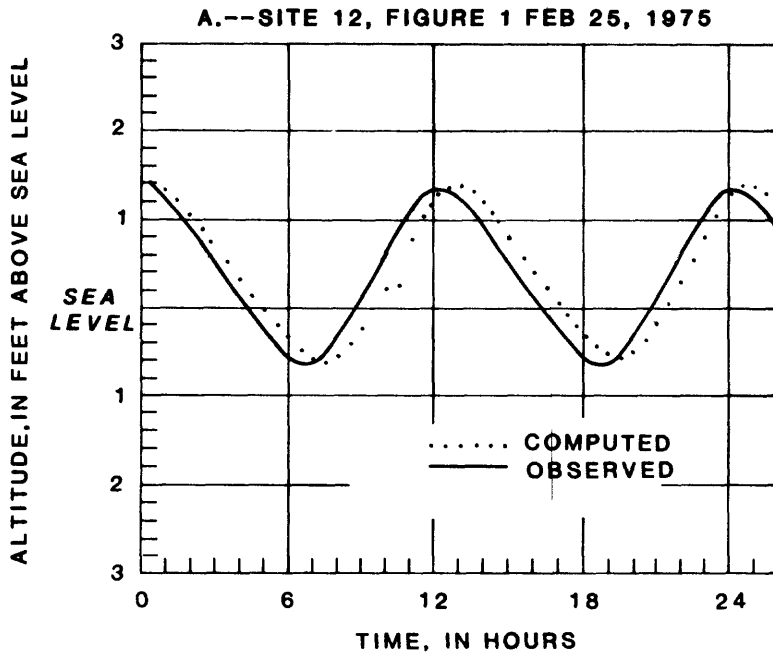


Figure 7.--Comparison of observed and computed tidal stage in the northwest fork and in the southwest fork, (A) site 12, (B) site 11.

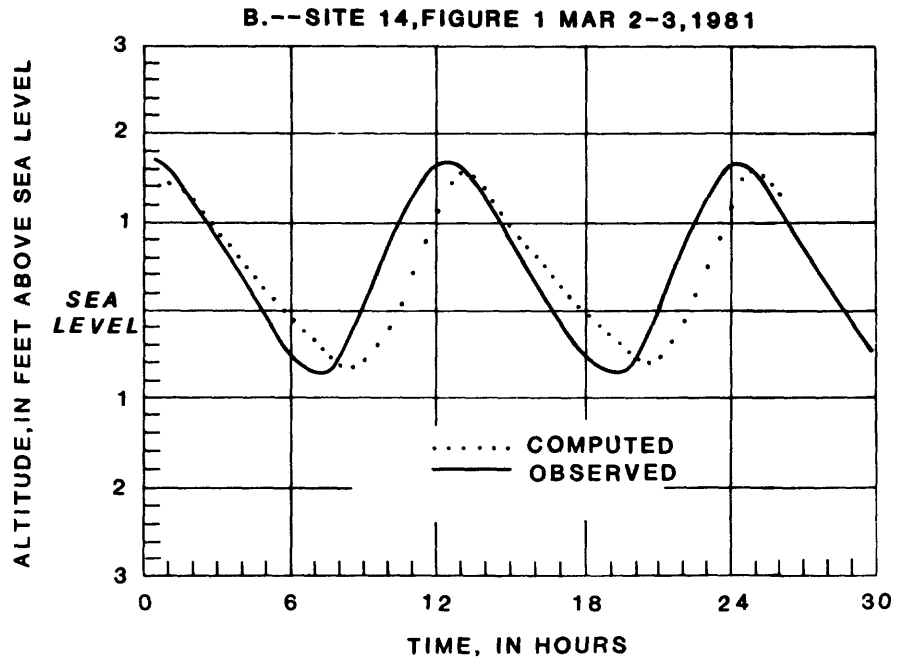
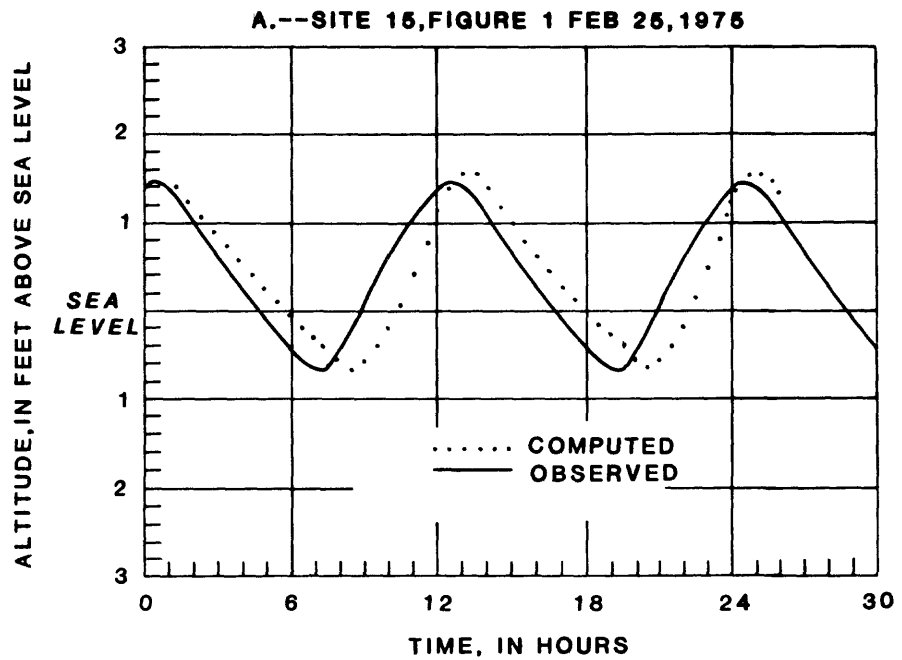


Figure 8.--Comparison of observed and computed tidal stage in the northwest fork, (A) site 15, (B) site 14.

Table 1.--Summary of comparisons between observed and computed tidal stage and tidal phase at high and low tides in the Loxahatchee River estuary

[Stage shown in feet above or below land surface;
phase lag from entrance shown in minutes]

Site number	Stage			Phase lag from entrance		
	Computed	Observed	Difference	Computed	Observed	Difference
<u>High tide (February 1975)</u>						
1	2.13	2.13	0.00	0	0	0
5	1.37	1.41	-.04	60	70	-10
8	1.40	1.44	-.04	85	85	0
12	1.37	1.38	-.01	170	130	40
¹ 15	1.60	1.49	-.11	212	306	94
<u>Low tide (February 1975)</u>						
1	-2.13	-2.13	.00	0	0	0
5	-.75	-.85	-.10	90	90	0
8	-.75	-.82	-.07	135	110	25
12	-.57	-.66	-.09	205	160	45
¹ 15	-.62	-.70	-.08	418	300	118

Site number	Stage			Phase lag from entrance		
	Computed	Observed	Difference	Computed	Observed	Difference
<u>High tide (March 1981)</u>						
4	1.37	1.50	-0.13	60	60	0
8	1.40	1.44	-.04	60	70	10
11	1.38	1.58	-.20	160	150	10
¹ 14	1.60	1.71	-.11	294	200	94
<u>Low tide (March 1981)</u>						
4	-.78	-.90	-.12	90	60	30
8	-.75	-.82	-.07	130	105	25
11	-.62	-.80	-.18	210	190	20
¹ 14	-.59	-.71	-.12	418	300	118

¹Difference values not used in average differences.

suggesting that the modeled freshwater inflow rates are higher than the prototype, or that numerical resolution of time or space is too coarse. Differences could also result because the narrow upstream river reaches were simulated using equivalent cross-sectional areas that had larger widths and shallower depths than the prototype. It is also possible that friction values chosen are too high in some areas.

Tidal Velocity

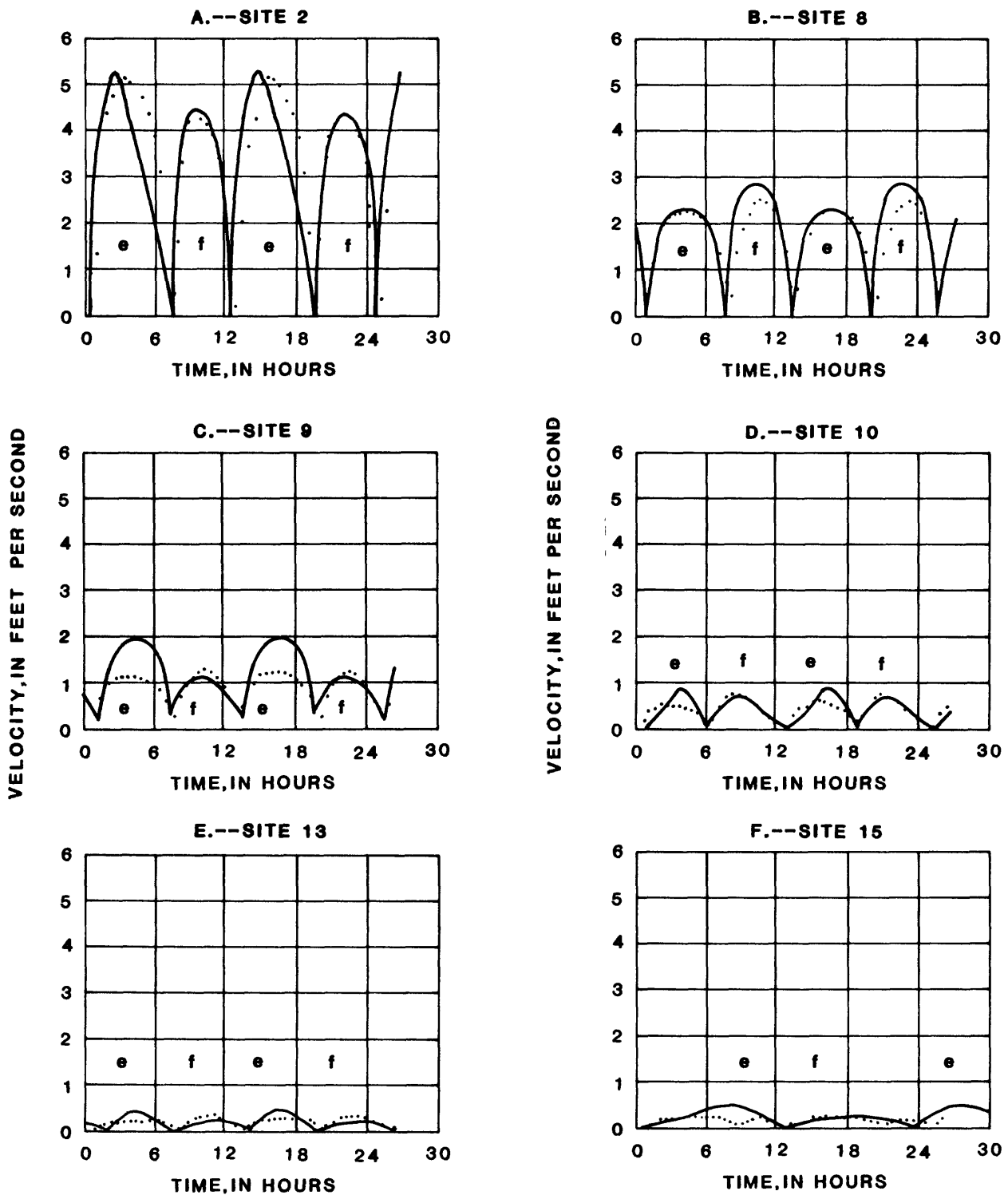
Comparisons of observed and computed tidal velocities were used as indicators of model calibration (fig. 9). Tidal velocities were measured at eight sites (fig. 1) by Chiu (1975). Each set of measurements represents the velocity at one location in a cross section and at a point about one-third of the depth above the bottom. Velocity data, therefore, do not represent cross-sectional averages that are subject to irregularities from shoals, bends, and scoured depressions. Also, the data do not cover a complete tide cycle; thus, some interpolation was necessary for slack-tide periods to provide complete data over a 12-hour tide cycle to correspond with model output data. Maximum velocities ranged from about 5 ft/s at site 2 (fig. 9A) in the inlet area to less than 0.5 ft/s at site 13 (fig. 9E) in the central embayment.

Distribution of Tidal-Flow Volumes

Assurance of model calibration in the Jupiter Inlet area was obtained by comparing measured and computed distributions of tidal-water flow to and from the inlet area (table 2). Tidal-flow measurements were computed from flow measurements at only one location in the cross section and do not cover a complete tide cycle. Comparisons of the percentages (table 2) are good and indicate that the model is well calibrated in the Jupiter Inlet area. The model defines the proper amount of water flowing to and from the central embayment, as indicated by measured and computed values at the FECRR bridge location (table 2).

Verification

The final step in model development usually is model verification. The objective of verification is to demonstrate how well the model can simulate conditions that are significantly different than those used for calibration. The verification procedure does not allow any additional adjustments to the model input data. Therefore, comparisons of observed and computed verification data serve as a check on the adequacy of the calibration procedure. Without verification, a model would be applicable to only those conditions for which it is calibrated. Fulfillment of study objectives could be met with a model that was calibrated using average freshwater-inflow rates and a representative, repeating, semidiurnal tide. Such data were available for use in model calibration, and additional data became available during the study period. Although the additional data show the model is capable of simulating conditions that are similar to those during the calibration period, simulation



EXPLANATION

- e**---PERIOD OF EBB FLOW
- f**---PERIOD OF FLOOD FLOW
- COMPUTED VALUE
- OBSERVED VALUE

Figure 9.--Comparison of observed and computed velocities, (A) site 2, (B) site 8, (C) site 9, (D) site 10, (E) site 13, (F) site 15.

Table 2.--Measured and computed distribution of tidal-flow volumes
in the vicinity of Jupiter Inlet

[Volume shown in cubic feet x 10⁸. NIWW, North Intracoastal Waterway;
SIWW, South Intracoastal Waterway; FECRR, Florida East Coast
Railroad; JI, Jupiter Inlet.]

Distribution	Flow measurement locations							
	NIWW		SIWW		FECRR		JI	
	Vol- ume	Per- cent	Vol- ume	Per- cent	Vol- ume	Per- cent	Vol- ume	
Measured: Chiu; 2/25/75								
Flood tide	¹ 1.33	45	¹ 0.32	11	¹ 1.28	44	2.93	
Ebb tide	--	--	--	--	--	--	--	
Computed: SIMSYS2D; 2/25/75								
Flood tide	.84	43	.20	10	.91	47	1.96	
Ebb tide	.95	45	.20	9	1.0	47	2.12	

¹Values judged to be high due to one section in cross section.

of another set of field conditions would require independent calibration and verification. Model results are, therefore, valid for calibration conditions only.

TIDAL FLOW AND CIRCULATION PATTERNS

The tidal flow and circulation patterns are presented as a series of computer-generated vector maps of the Loxahatchee River estuary. Vector lengths are proportional to their magnitude of the velocity and are shown as straight lines without arrowheads. Vectors which occasionally transgress land boundaries are indicative of transport magnitude and not of water transport over land surface. Vector angles may be determined by the direction from which the vector emanates from a small square at the center of alternate cells. Minute nonzero vectors appear as a dot or a small square without any line.

For this report, water transport is defined as a vector quantity that represents the average rate of water flow through a cell during a 30-minute period. Residual water transport is defined as a vector quantity that represents the net rate of water flow through a cell during a 12-hour repeating tidal cycle. The following sections describe computed ebb, flood, near-slack, and residual water-transport patterns in the central embayment and inlet regions of the Loxahatchee River estuary.

Ebb Transport

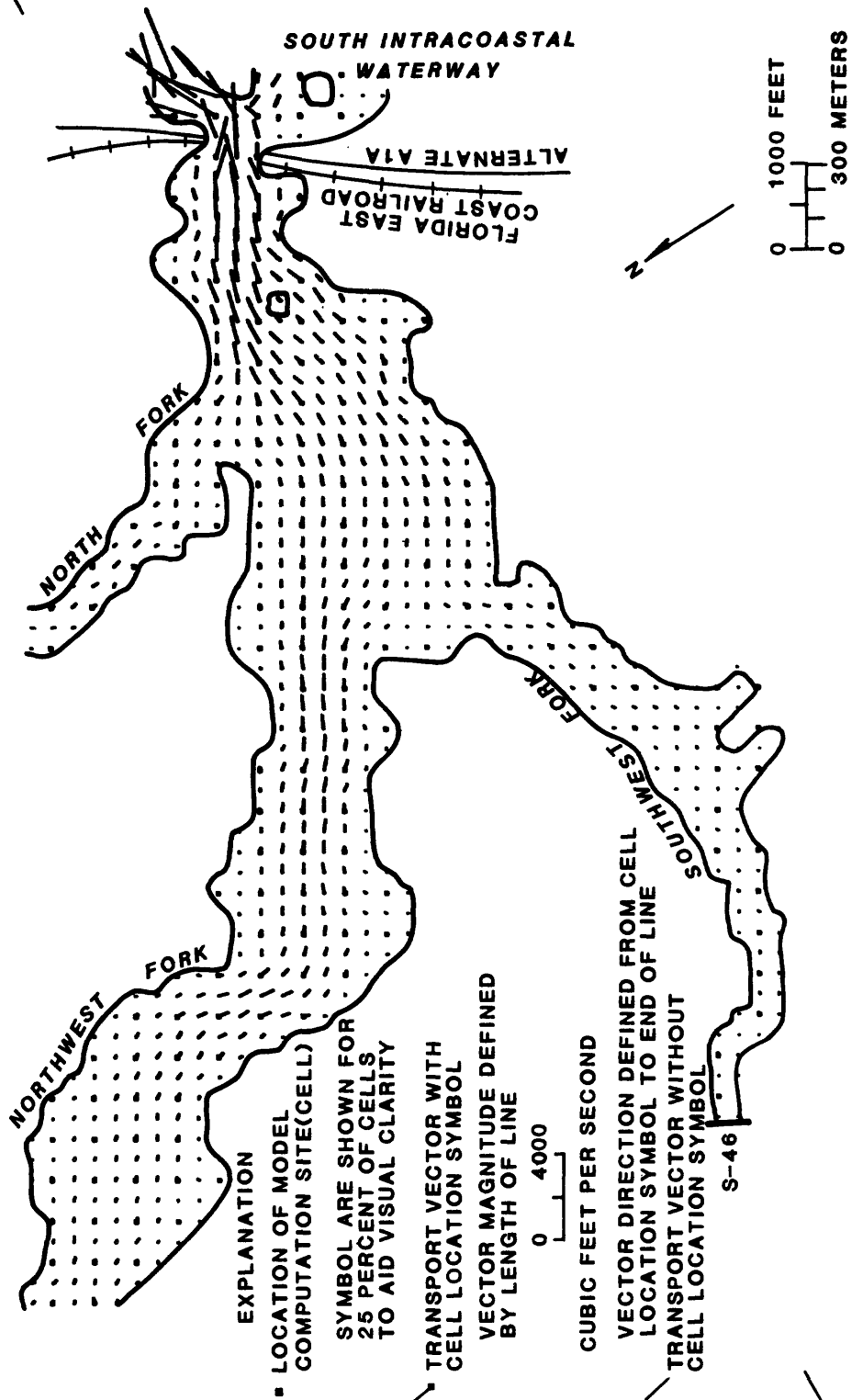
Figures 10 and 11 show computed ebb-tide water-transport patterns in the central embayment and from Jupiter Inlet to the central embayment, respectively. In the central embayment, ebb-transport vectors are largest at the seaward end where the channel becomes constricted just west of the FECRR bridge. Throughout the widest part of the embayment (fig. 10), ebb-transport rates at each cell are nearly uniform at about 500 ft³/s; they are slightly higher in the lower reaches of the northwest fork. Ebb-transport rates in the north fork, southwest fork, and upper parts of the northwest fork are generally less than 200 ft³/s at most cells.

Figure 11 shows ebb-flow patterns from the seaward end of the central embayment, through Jupiter Inlet, and into the Atlantic Ocean. The pattern indicates large transport rates, many greater than 3,000 ft³/s, flowing toward the inlet from the central embayment and the North Intracoastal Waterway. Transport rates in the South Intracoastal Waterway are generally less than 500 ft³/s at most cells. The largest transport rates (greater than 6,000 ft³/s) occur at Jupiter Inlet just before entering the ocean. Offshore transport rates are quickly reduced as flow is spread over a large ocean area. Offshore flow patterns seem to be influenced by extensive sandbars.

Flood Transport

Figures 12 and 13 show computed flood-tide water-transport patterns in the central embayment and inlet regions, respectively. The patterns are

80° 07'



26° 57'

Figure 10.--Water transport in the central embayment during ebb tide.

80° 05'

EXPLANATION

■ LOCATION OF MODEL COMPUTATION SITE (CELL)

SYMBOL ARE SHOWN FOR 25 PERCENT OF CELLS TO AID VISUAL CLARITY

TRANSPORT VECTOR WITH CELL LOCATION SYMBOL

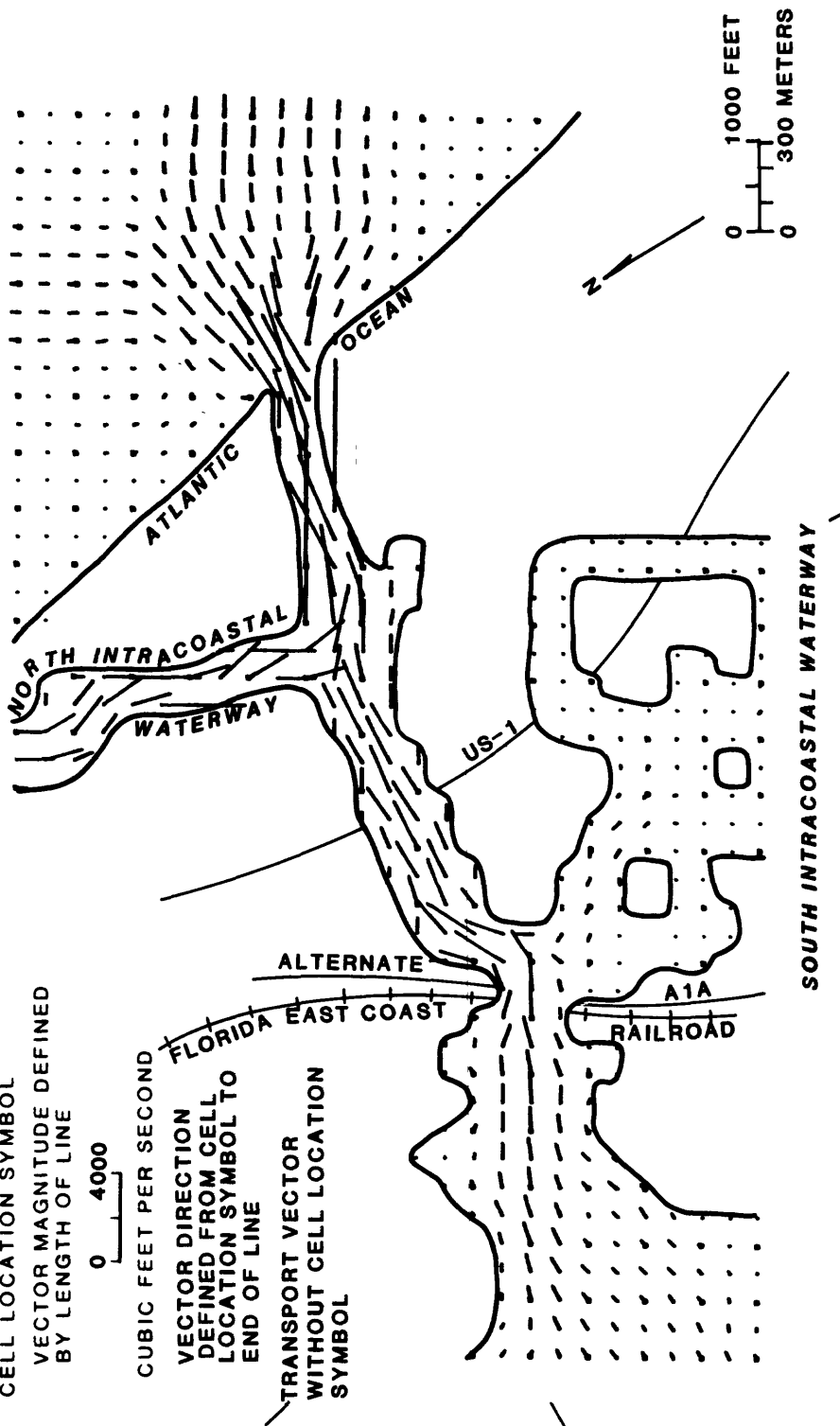
VECTOR MAGNITUDE DEFINED BY LENGTH OF LINE

0 4000

CUBIC FEET PER SECOND

VECTOR DIRECTION DEFINED FROM CELL LOCATION SYMBOL TO END OF LINE

TRANSPORT VECTOR WITHOUT CELL LOCATION SYMBOL



26° 57'

Figure 11.--Water transport from Jupiter Inlet to the central embayment during ebb tide.

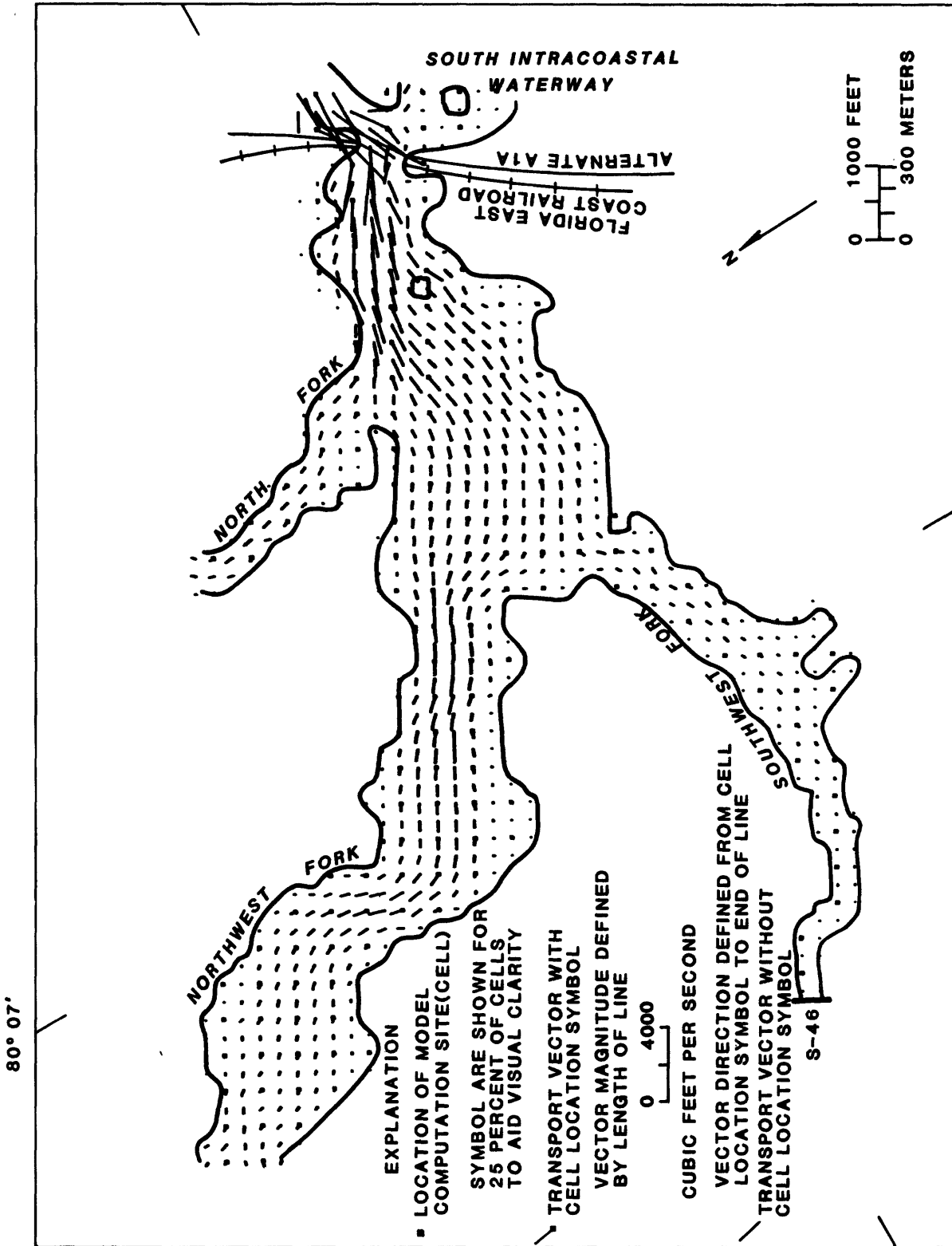


Figure 12.--Water transport in the central embayment during flood tide.

80° 05'

26° 57'

EXPLANATION

■ LOCATION OF MODEL COMPUTATION SITE (CELL)

SYMBOL ARE SHOWN FOR 25 PERCENT OF CELLS TO AID VISUAL CLARITY

TRANSPORT VECTOR WITH CELL LOCATION SYMBOL

VECTOR MAGNITUDE DEFINED BY LENGTH OF LINE

0 4000

CUBIC FEET PER SECOND

VECTOR DIRECTION DEFINED FROM CELL LOCATION SYMBOL TO END OF LINE

TRANSPORT VECTOR WITHOUT CELL LOCATION SYMBOL

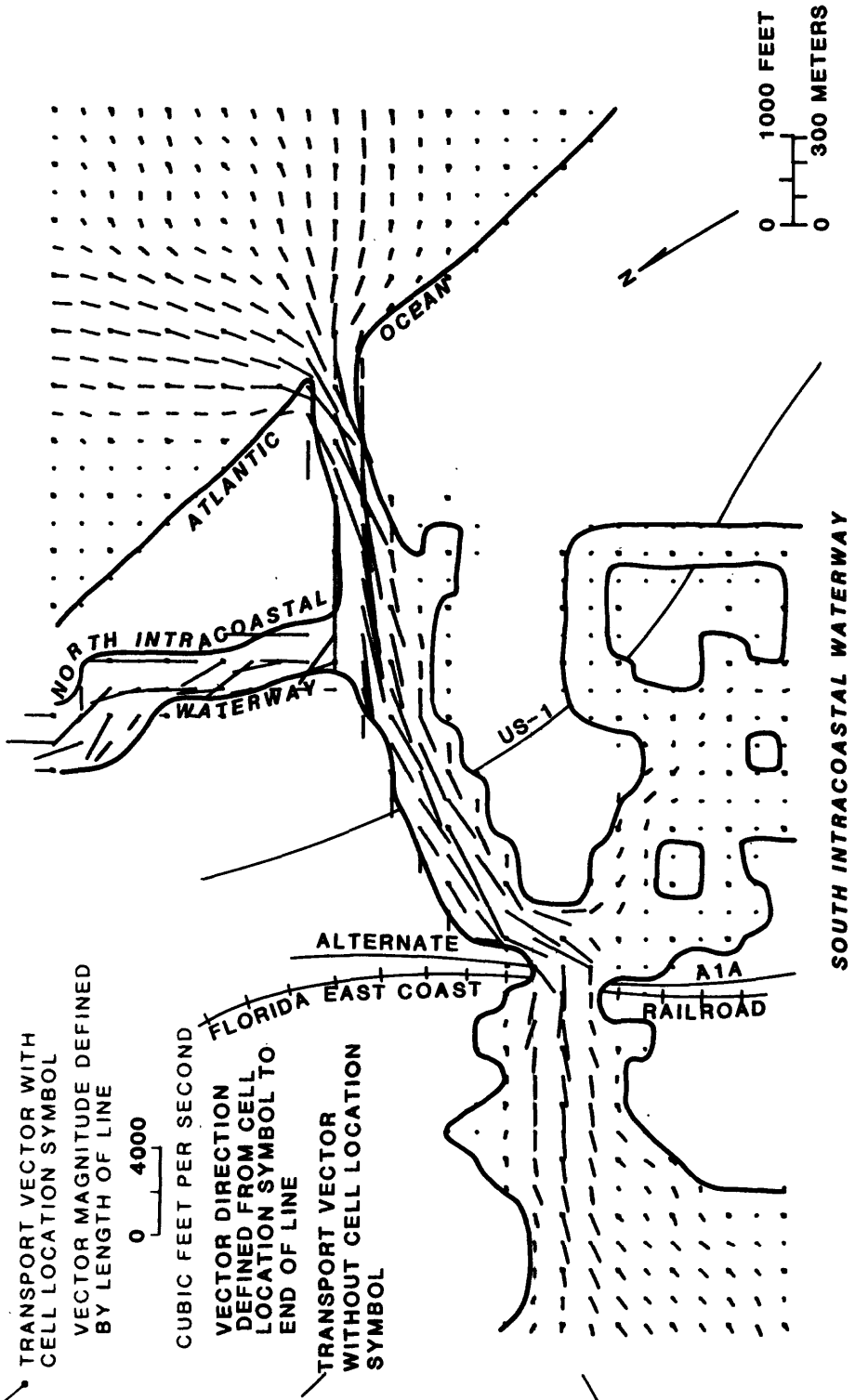


Figure 13. --Water transport from Jupiter Inlet to the central embayment during flood tide.

analogous to those in figures 10 and 11 except that flow is into the estuary instead of outward. No substantial differences between ebb- and flood-transport patterns are evident except perhaps in the ocean where southward-flowing transport vectors are larger (fig. 13) than northward-flowing vectors (fig. 11).

Near-Slack Transport

Figures 14 and 15 show computed near-slack tide water-transport patterns in the central embayment and inlet regions, respectively. Allowing for the difference in transport scales, flow conditions in the inlet region (fig. 15) and in the central embayment (fig. 14) can be compared. Outward flow predominates in the ocean at the mouth of Jupiter Inlet and at much lower velocities in the South Intracoastal Waterway (fig. 15). A region of random, and possibly rotational, flow occurs within the inlet and in part of the North Intracoastal Waterway (fig. 15). Flow is generally inward throughout the central embayment but is mostly confined to deep areas (fig. 14).

The random flow pattern within the inlet area indicates that mixing often occurs during slack and near-slack conditions. The hydraulic situation can be described as a period of instability when tidal water-level gradients are too weak to organize the flow. In the central embayment, water flowing in the deeper areas has greater inertia than water flowing in adjacent shallow areas. This inertia tends to keep the deeper water flowing after adjacent water has either stopped flow or the flow has reversed in response to tidal water-level gradients.

Residual Transport

Residual water transport is the resultant vector of the arithmetic sum of all north-south flow components combined with the arithmetic sum of all east-west flow components that pass a given cell during one complete repeating tide cycle. Residual transport maps that depict long-term circulation patterns in the central embayment and inlet areas are shown in figures 16 and 17.

Circulation patterns in the central embayment seem to be dominated by the effects of freshwater flowing through the estuary to the ocean. Little indication of tide-induced circulation features can be seen in figure 16, except possibly for localized gyres in the lower reaches of the north and southwest forks. Seaward-flowing residual transport vectors between 50 and 100 ft³/s seem to follow river meanders and natural channels in the northwest fork. The flow is distributed almost evenly across the widest part of the central embayment. Near the western end of the embayment where the northwest fork begins, the flow is concentrated in natural and dredge channels.

Residual transport in the vicinity of Jupiter Inlet (fig. 17) is dominated by seaward flow in the inlet channel and the North Intracoastal Waterway. Computations also show a large counterclockwise circulating gyre in the Atlantic Ocean, which may possibly be induced by boundary conditions of the model rather than the strong outward current emanating from the inlet.

80° 07'

26° 57'

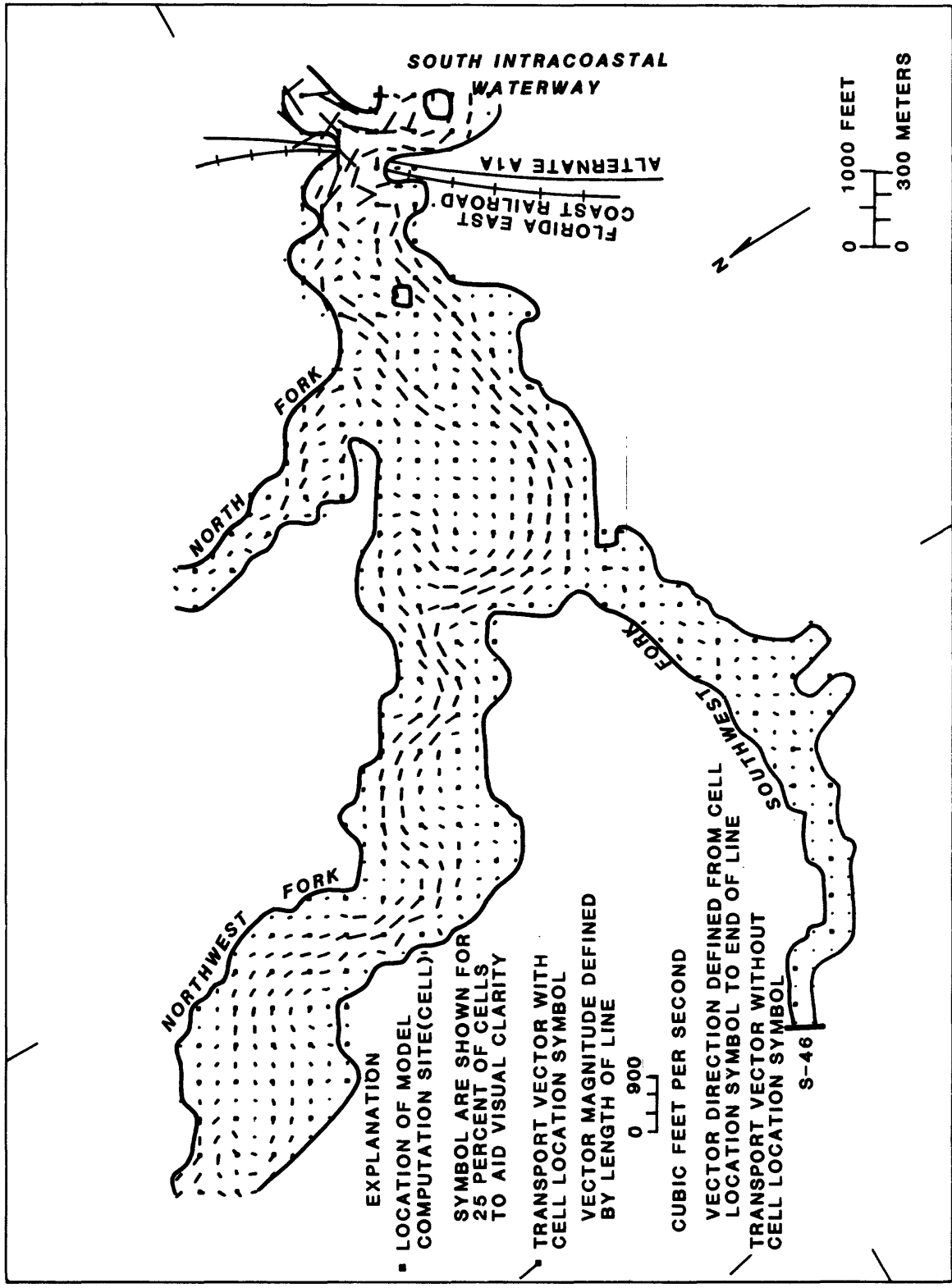


Figure 14.--Water transport in the central embayment during near-slack tide.

80° 05'

EXPLANATION

■ LOCATION OF MODEL COMPUTATION SITE (CELL)

SYMBOL ARE SHOWN FOR 25 PERCENT OF CELLS TO AID VISUAL CLARITY

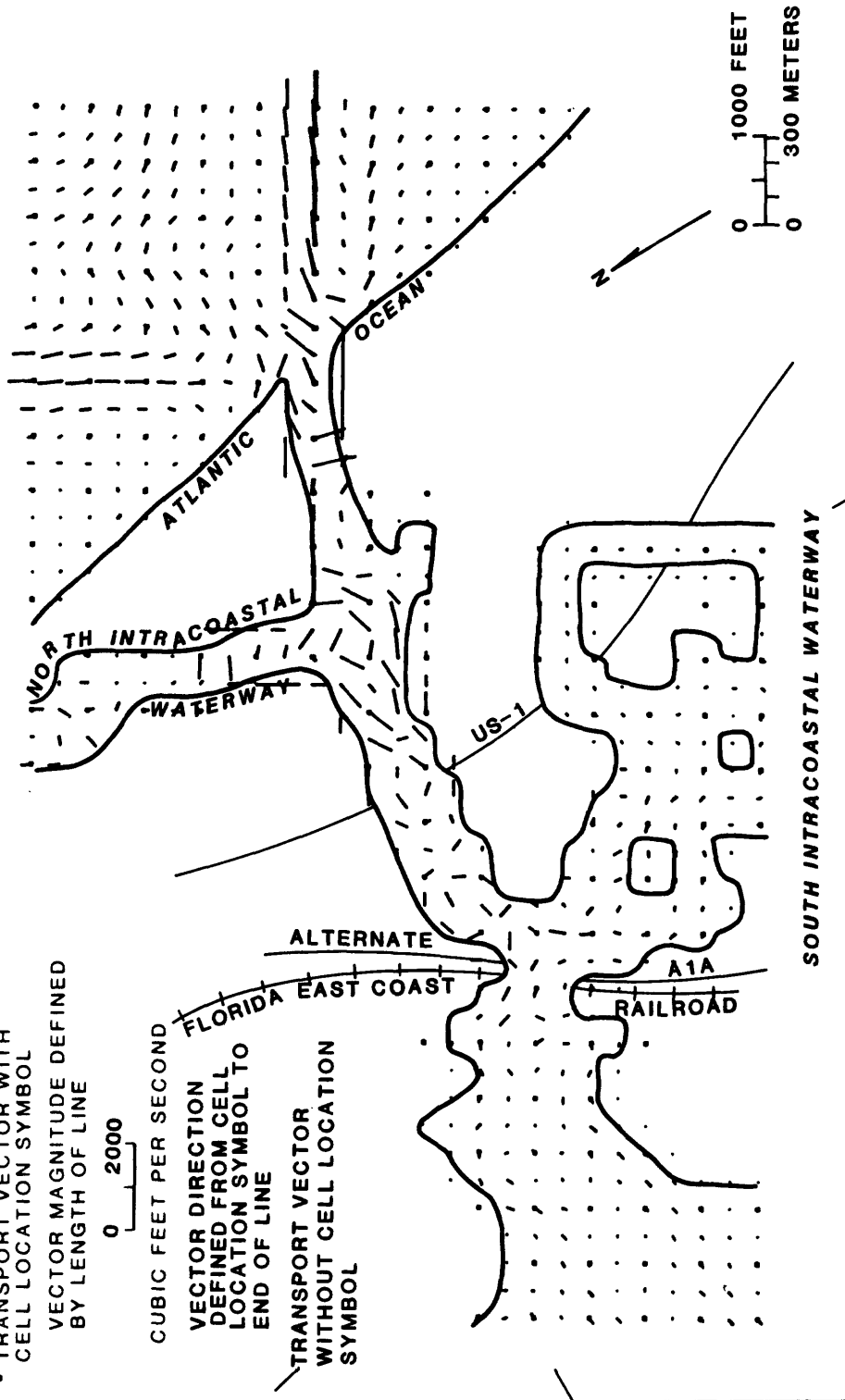
TRANSPORT VECTOR WITH CELL LOCATION SYMBOL
VECTOR MAGNITUDE DEFINED BY LENGTH OF LINE

0 2000

CUBIC FEET PER SECOND

VECTOR DIRECTION DEFINED FROM CELL LOCATION SYMBOL TO END OF LINE

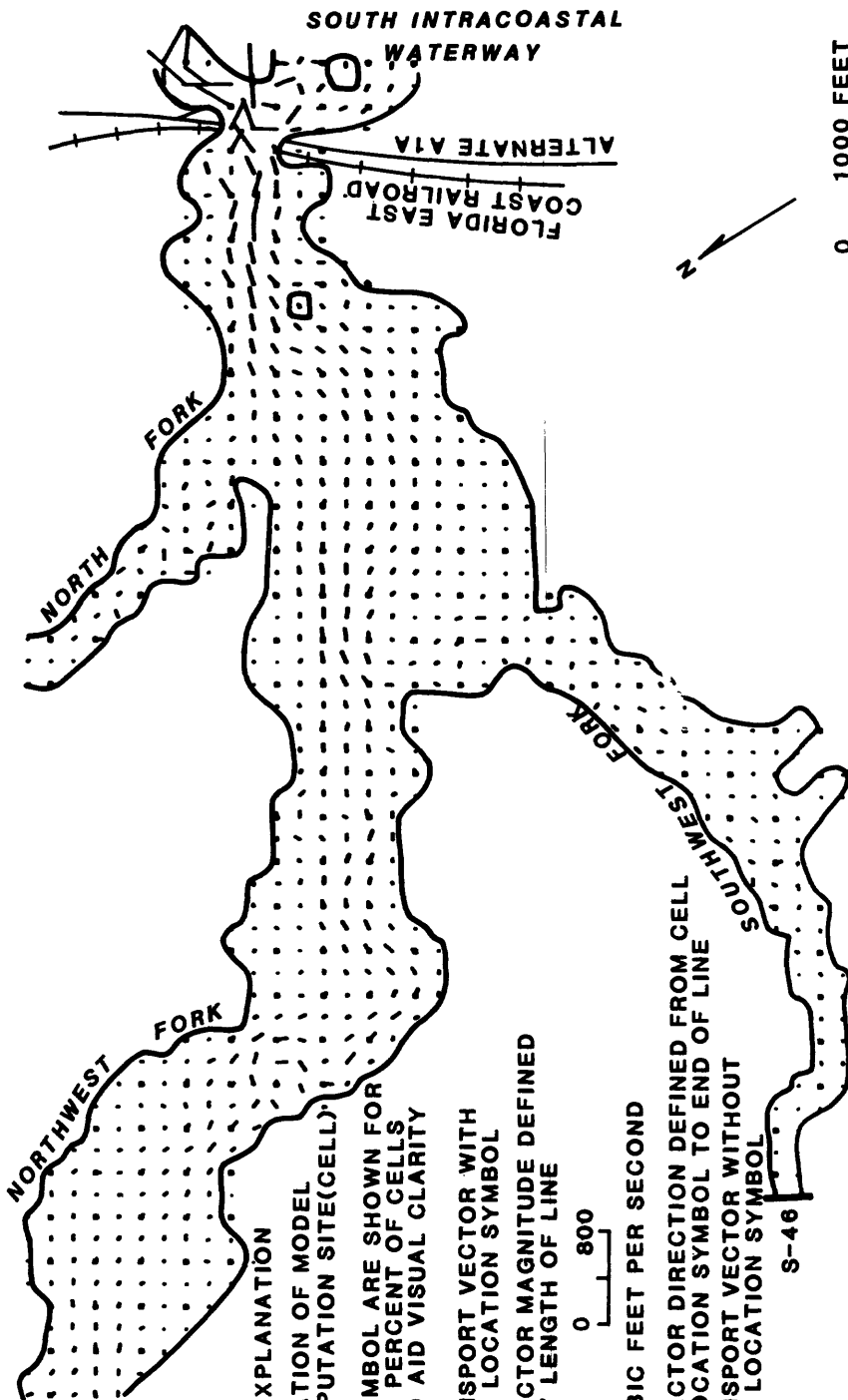
TRANSPORT VECTOR WITHOUT CELL LOCATION SYMBOL



26° 57'

Figure 15.--Water transport from Jupiter Inlet to the central embayment during near-slack tide.

80° 07'



EXPLANATION

▣ LOCATION OF MODEL COMPUTATION SITE(CELL)

• SYMBOL ARE SHOWN FOR 25 PERCENT OF CELLS TO AID VISUAL CLARITY

—▶ TRANSPORT VECTOR WITH CELL LOCATION SYMBOL
—• VECTOR MAGNITUDE DEFINED BY LENGTH OF LINE

0 800

CUBIC FEET PER SECOND

—▶ VECTOR DIRECTION DEFINED FROM CELL LOCATION SYMBOL TO END OF LINE
—• TRANSPORT VECTOR WITHOUT CELL LOCATION SYMBOL

S-46

0 1000 FEET
0 300 METERS



26° 57'

Figure 16.--Residual water transport in the central embayment.

80° 05'

EXPLANATION

■ LOCATION OF MODEL COMPUTATION SITE(CELL)

SYMBOL ARE SHOWN FOR 25 PERCENT OF CELLS TO AID VISUAL CLARITY

TRANSPORT VECTOR WITH CELL LOCATION SYMBOL

VECTOR MAGNITUDE DEFINED BY LENGTH OF LINE

0 1000

CUBIC FEET PER SECOND

VECTOR DIRECTION DEFINED FROM CELL LOCATION SYMBOL TO END OF LINE

TRANSPORT VECTOR WITHOUT CELL LOCATION SYMBOL

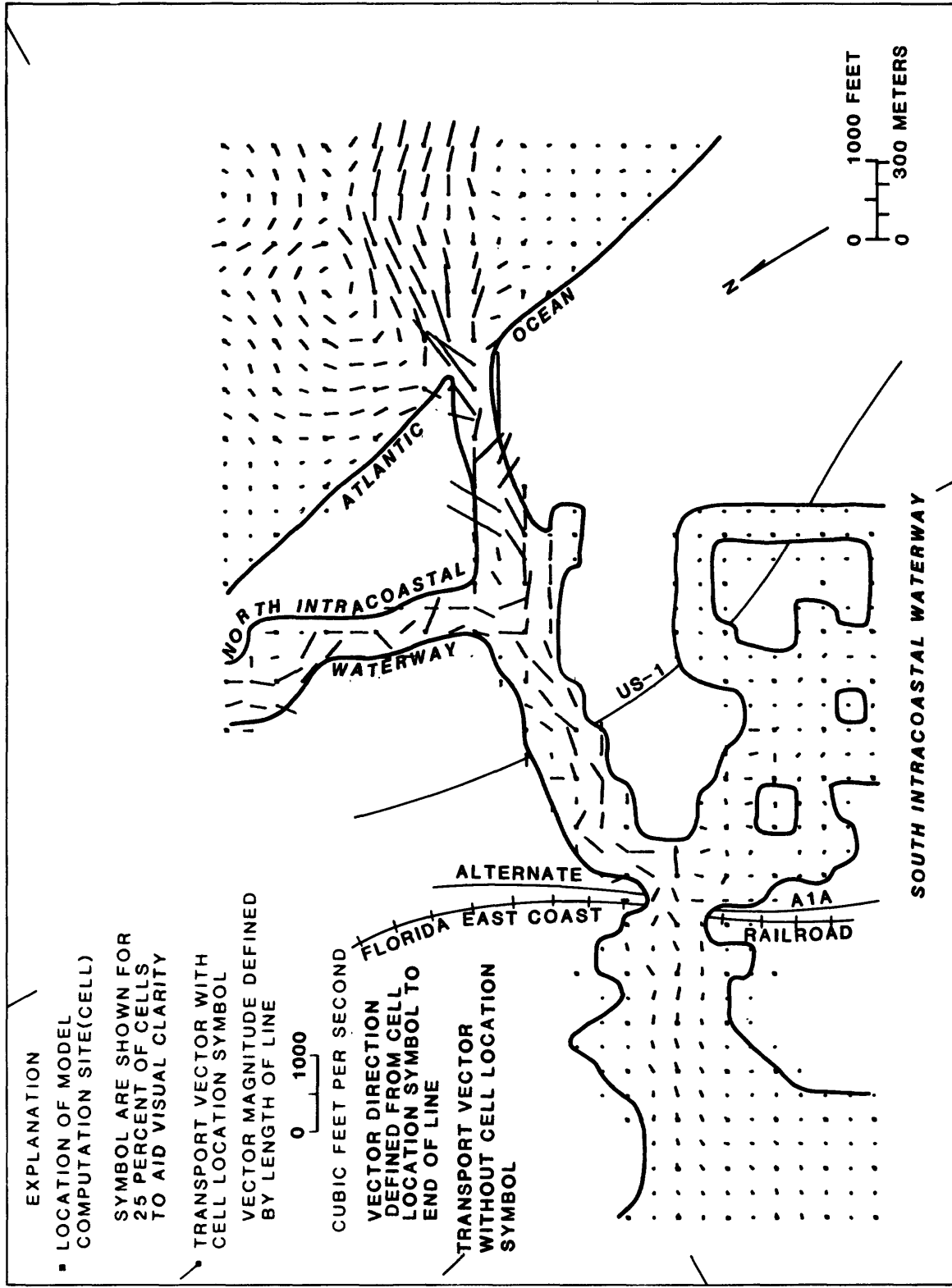


Figure 17.--Residual water transport from Jupiter Inlet to the central embayment.

Because of narrow channel widths and the 250-foot grid size, detection of circulation features within the inlet channel and connecting waterways is difficult. Landward-flowing residual vectors occur at some cells within the inlet channel and connecting waterways. These landward-flowing residual vectors may indicate localized tide-induced circulation and mixing.

SUMMARY AND CONCLUSIONS

The SIMSYS2D (a two-dimensional estuarine-simulation system) was applied to the Loxahatchee River estuary system including Jupiter Inlet, the North Intracoastal Waterway, the South Intracoastal Waterway, the central embayment, and three tributary streams. The model was calibrated using existing and new tidal-stage data, existing tidal-velocity data, and existing and new information on the distribution of tidal-flow volumes. Calibration results indicated similarity between observed and computed tidal-stage and phase data except in the upper reaches of the estuary. Tidal-velocity and tidal-flow volume comparisons also indicated similarity between observed and computed data.

Maximum stage and phase differences between model and prototype data were about 0.20 foot and 45 minutes, respectively, and occurred in the upper reaches of the modeled area. The differences were probably the result of model sensitivity to streamflow and possibly a model grid size of 250 feet that did not allow adequate spatial resolution of the tidal wave.

Results indicate that the model can simulate tidal-water motion in the estuary for vertically well-mixed conditions. Typical flow patterns during flood and ebb tides show high water-transport rates (more than 6,000 ft³/s) near the inlet channel and in the North Intracoastal Waterway. Lower transport rates, less than 1,000 ft³/s, were computed in most other parts of the estuary. The central embayment has a nearly even distribution of flow across the widest section during flood and ebb tides. During slack tide, a random flow pattern occurs in the inlet channel, which may indicate a higher degree of mixing.

Residual transport patterns in the central embayment showed a dominance of freshwater-induced circulation over tide-induced circulation. Residual transport in the vicinity of Jupiter Inlet is dominated by seaward flow in the inlet channel and the North Intracoastal Waterway.

The model can simulate tidal flow and circulation in the Loxahatchee River estuary under typical low freshwater inflow and vertically well-mixed conditions. An investigation of the effects of various physical changes to the estuary such as channel dredging, shoal removal, and entrance closure can be undertaken using this model. Results of such work will be limited, however, to low-flow and well-mixed conditions. Model investigations of partly mixed or stratified conditions in the estuary need to await development of systems capable of simulating three-dimensional flow patterns.

REFERENCES CITED

- Barnes, H.H., Jr., 1967, Roughness characteristics of natural channel: U.S. Geological Survey Water-Supply Paper 1849, 213 p.
- Chiu, T.Y., 1975, Evaluation of salt intrusion in Loxahatchee River, Florida: University of Florida Coastal and Oceanographic Engineering Laboratory UFL/COEL-75/013, 49 p.
- Goodwin, C.R., 1977, Circulation patterns for historical, existing, and proposed channel configurations in Hillsborough Bay, Florida: International Navigation Congress, 24th Proceedings, 13 p.
- 1980, Preliminary simulated tidal flow and circulation patterns in Hillsborough Bay, Florida: U.S. Geological Survey Open-File Report 80-1021, 25 p.
- Leendertse, J.J., 1970, A water-quality simulation model for well-mixed estuaries and coastal seas, Volume I, Principles of computation: Santa Monica, Calif., The Rand Corporation Publication RM-6230, 71 p.
- Leendertse, J.J., and Gritton, E.C., 1971, A water-quality simulation model for well mixed estuaries and coastal seas, Volume II, Computational procedures: Santa Monica, Calif., The Rand Corporation Publication R-708-NYC, 55 p.
- McPherson, B.F., and Sabanskas, Maryann, 1980, Hydrologic and land-cover features of the Loxahatchee River basin, Florida: U.S. Geological Survey Water-Resources Investigations Open-File Report 80-1109, 1 sheet.
- McPherson, B.F., Sabanskas, Maryann, and Long, W.A., 1982, Physical, hydrological, and biological characteristics of the Loxahatchee River estuary, Florida: U.S. Geological Survey Water-Resources Investigations Open-File Report 82-350, 1 sheet.
- McPherson, B.F., and Sonntag, W.H., 1983, Sediment and nutrient loads associated with a tropical storm, Loxahatchee River estuary, southeastern Florida: Coastal Zone '83, v. III, p. 2250.
- 1984, Transport and distribution of nutrients in the Loxahatchee River estuary, southeastern Florida, 1979-81: American Water Resources Association Bulletin, v. 20, no. 1, p. 27-34.
- McPherson, B.F., Sonntag, W.H., and Sabanskas, Maryann, 1984, Fouling community of the Loxahatchee River estuary, Florida, 1980-81: Estuaries, v. 7, no. 2, p. 149-157.
- Russell, G.M., and McPherson, B.F., 1983, Freshwater runoff and salinity distribution in the Loxahatchee River estuary, southeastern Florida, 1980-82: U.S. Geological Survey Water-Resources Investigations Report 83-4244, 36 p.
- Sonntag, W.H., and McPherson, B.F., 1984a, Nutrient input from the Loxahatchee River Environmental Control District sewage-treatment plant to the Loxahatchee River estuary, southeastern Florida: U.S. Geological Survey Water-Resources Investigations Report 84-4020, 23 p.
- 1984b, Sediment concentrations and loads in the Loxahatchee River estuary, Florida, 1980-82: U.S. Geological Survey Water-Resources Investigations Report 84-4157, 30 p.
- Wanless, Harold, Rossinsky, Victor, Jr., and McPherson, B.F., 1984, Sedimentologic history of the Loxahatchee River estuary, Florida: U.S. Geological Survey Water-Resources Investigations Report 84-4120, 58 p.

GLOSSARY

Boundary conditions.--Data that define conditions existing at the various model boundaries for the duration of the computational period.

Initial conditions.--Data that define the physical characteristics of water within the estuary and its condition at the start of the computational period.

Residual water transport.--Vector quantity that represents the net rate of water flow through a cell during a 12-hour repeating tidal cycle.

Water transport.--Vector quantity that represents the average rate of water flow through a cell during a 30-minute period.